

Evolution of dynamic flow behavior in asphalt mixtures exposed to freeze-thaw cycles

Xu Huining^{a,*}, Shi Hao^a, Zhang Huanyu^a, Li Hengzhen^a, Leng Zhen^b, Tan Yiqiu^{a,c}

^a School of Transportation Science and Engineering, Harbin Institute of Technology, Harbin 150090, China

^b Department of civil and environmental engineering, Hong Kong Polytechnic University, Hongkong 810005, China

^c State Key Laboratory of Urban Water Resource and Environment, Harbin Institute of Technology, Harbin 150090, China

*Corresponding author:

Huining Xu

School of Transportation Science and Engineering, Harbin Institute of Technology, Harbin 150090, China

Tel: +86-451-86282120

Fax: +86-451-86283090

E-mail: xuhn@hit.edu.cn

1 **Highlights**

- 2 ● Evolution of dynamic flow in asphalt mixture under freeze-thaw cycles is studied with X-ray CT
- 3 ● Freeze-thaw cycles increase the wetting front penetration depth and velocity for vertical flow
- 4 ● Freeze-thaw cycles have a positive effect on the vertical seepage velocity growth rate
- 5 ● For asphalt mixtures with small pore size, the vertical seepage velocity growth rate rises more
- 6 rapidly

7 **Abstract:** This study aims to understand the evolution of dynamic moisture flow in asphalt mixtures
8 exposed to freeze-thaw cycles. X-ray CT was utilized to capture the moisture dynamics in
9 unsaturated asphalt mixtures during simulated rainfall events. Three main characteristics of the
10 dynamic flow behaviors within asphalt mixtures were measured and monitored, including: wetting
11 front position, directional velocity of wetting front, and inertia influence region. It was found that
12 at a specific infiltration rate, freeze-thaw cycles increased the vertical flow penetration and
13 decreased the horizontal flow penetration for both wetting front position and directional velocity,
14 suggesting that seepage anisotropy was exacerbated in asphalt mixtures. The initial inertia of water
15 droplet was mostly converted towards the vertical direction under freeze-thaw effect. As a result,
16 the shape of water transmission was converted from a hemispherical shape to a slender shape under
17 freeze-thaw cycles. Linear regression analysis between direction velocity growth rate in particular
18 samples and freeze-thaw cycles to pore structure was conducted, and it was found that compared
19 with dense-graded mixtures, open-graded mixtures displayed larger slopes for horizontal flow, and
20 smaller slopes for vertical flow, demonstrating the non-negligible effect of pore structure on
21 dynamic flow evolution under freeze-thaw cycles.

22 **Keyword:** Asphalt mixture; Freeze-thaw cycle; Wetting front; Local velocity; Initial inertial region

1 **Introduction**

2 Asphalt mixture is a special porous medium consisted of asphalt binder, aggregate, and air void,
3 which is widely used in pavement engineering [1]. The role of moisture in pore structure and its
4 transport phenomena occurring in asphalt mixtures have long been recognized, and during the last
5 20 years, many studies have been conducted on freeze-thaw damage of asphalt mixtures in cold
6 regions caused by existence of moisture [2-5]. Moisture transport in asphalt mixtures has been
7 mainly analyzed using Darcy's law and Kozeny-Carman formulation [6], and non-equilibrium
8 equations such as dual permeability have been developed to describe the moisture transmission in
9 large pore size [7-10]. These macroscopic analysis approaches are helpful in determining the
10 permeability coefficient and flow regime, but they still suffer from a lack of explicit links with the
11 pore structure features in asphalt mixtures [11-14]. Especially, under the cyclic freeze-thaw action,
12 the pore structure in asphalt mixture is degraded dynamically, and the time-varying pore structure
13 provides more flow paths for moisture transport [15, 16]. Therefore, the moisture distribution in
14 asphalt mixture with exposure to freeze-thaw cycles is a dynamic process. Up to now, such process
15 was often conducted with experimental analysis from macro aspect before and after freeze-thaw
16 cycles. The obtained experimental data was always used to match theoretical equations [2].

17 Recently, Conte and Ferro [16], Kruse et al. [17], Masad et al. [19] and Xu et al. [20] proposed
18 a new method to assess the micro-scale moisture distribution in pavement on the basis of the
19 processing of microscopic testing techniques, such as X-ray computed tomography (CT) and nuclear
20 magnetic resonance. Although these approaches proved only able to quantify an average state within
21 a specific time interval, they are promising because the moisture distribution can be directly
22 measured instead of being predicted from data fitting or inverse modeling. However, these

1 approaches cannot account for the dynamic moisture transport process, which is ubiquitous in
2 asphalt mixture [21-23]. As pointed out by Vardanega [24] and Guo [25], there are still unanswered
3 fundamental questions about moisture in asphalt mixtures, such as “How does wetting front pass
4 through pore structure in asphalt mixtures?” and “How does moisture in asphalt mixtures interact
5 with pore structure in asphalt mixture exposed to environmental load and vehicle load?”. Therefore,
6 new developments in experiment and analysis methods are needed to approach these questions.

7 For the past few years, X-ray CT has been successfully applied as a tool in the microscale
8 analysis of porous mediums. This technique is based on the X-ray spectrometer to image the internal
9 microscale structure of objects without destruction. To date, however, in the asphalt mixture studies
10 at microscale, the X-ray CT was mainly dedicated to the characterization of pore structure of
11 particular samples or to monitor structure evolution under various external factors [26-28]. X-ray
12 CT is less extensively used as a nondestructive approach to image the inner structure of asphalt
13 mixtures, combining moisture, aggregate, and voids. Khan et al. [29] pointed that the three-
14 dimensional mapping of the attenuation coefficients obtained in asphalt mixtures is well adapted to
15 detect moisture in asphalt mixtures, and can be used in imaging microscale moisture distribution
16 inside asphalt mixture. Jerjen et al. [30] performed a drying test utilizing the similar approach with
17 open-graded asphalt mixture. Xu et al. [31] proposed a method, named non-void object increment
18 approach, to distinguish the moisture from the base of asphalt mixture. This approach could image
19 the distribution of water flow in a particular slice inner sample. Compared with the previous
20 approaches, the non-void object increment method illustrated a significant improvement in the
21 accuracy of moisture content. However, the non-void object increment method is very time-
22 consuming, which takes 30-45 min for a sample. Xu et al. [31] proposed a new algorithm for the

determination of wetting front in sample with X-ray CT and provide a practical way for the analysis of dynamic movements of moisture in asphalt mixtures. With respect to these new technical advances, two points may be highlighted: (i) most of the studies imaging the spatial distributions of moisture in asphalt mixtures were essentially conducted under stationary flow, and few focused on the dynamic flow; (ii) the seepage characteristic of asphalt mixtures is structure-dependent, which varies with the action of external environment, such as freeze-thaw cycles.

Hence, the objective of this study is to track the moisture flow path and reveal the evolution of dynamic flow inside the samples under exposure with freeze-thaw cycles by adopting a three-dimensional X-ray CT technology. Three common types of asphalt mixtures were evaluated. The dynamic flow behaviors, such as penetration depth, penetration rate, inertia influence region (IIR) and inertia non-influence region (INR) under various infiltration rates in asphalt mixtures were analyzed. Thereafter, the freeze-thaw cycles were applied to the samples. And the samples suffered from 3, 6, and 9 freeze-thaw cycles respectively were tested with X-ray CT to analyze the change in flow behaviors. Evolution in penetration rate and IIR were used to evaluate the effect of freeze-thaw cycles on the dynamic flow behaviors in asphalt mixtures. In addition, the variations in dynamic flow characteristics were observed among different types of asphalt mixtures to illustrate the role of pore structure on seepage characteristic evolution with freeze-thaw cycles.

Material and methods

Samples

Two dense-graded asphalt mixtures and one open-graded asphalt mixture, namely asphalt concrete (AC), stone matrix asphalt (SMA), open graded friction concrete (OGFC), respectively, were produced in the lab to study the flow dynamics with exposure to freeze-thaw cycles. The

1 nominal maximum aggregate size for all samples was 13.2 mm. Following the Technical
2 Specification for Construction of Highway Asphalt Pavements (JTG F40-2004), the target air void
3 content was $4.0\pm1\%$ for AC and SMA mixtures, $18.0\pm1\%$ for OGFC mixture. And the designed
4 height of samples was $63.5\pm1.3\text{mm}$, designed diameter was $100\pm0.2\text{mm}$. The penetration grade of
5 asphalt binder was 80/100. Andesite aggregate collected at local aggregate plant in Heilongjiang
6 Province was used to prepare the samples. Lignin fiber was used in SMA with a mass content of
7 3‰.

8 Superpave gyratory compactor was adopted to compact the samples with a standard vertical
9 pressure (0.6MPa), gyration angle (1.25°), and gyration speed (30 rpm). Four replicate samples for
10 each mixture type were fabricated to demonstrate the evolution of moisture transport characteristics
11 in different samples under freeze-thaw cycles.

12 *Seepage experimental setup*

13 In order to describe the water flow behavior inside the asphalt mixture, Xu et al [31] developed
14 a seepage experiment utilizing a micro medical syringe pump with accuracy of 0.1ml/min. The
15 needle of syringe pump was fixed in the center of sample's upper surface. The syringe pump was
16 connected with a water tank to supply the pressured water and water flow is calibrated. This seepage
17 experimental method was also employed in this study.

18 *Freeze-thaw experimental procedure*

19 The freeze-thaw test method according to the Standard Test Methods of Bitumen and
20 Bituminous Mixtures for Highway Engineering (E20-2011) was used to simulate the micro structure
21 damages from hoarding moisture in asphalt mixture under the positive and negative temperature
22 alternation. In a freeze-thaw cycle, all the asphalt mixture samples were first treated in the distilled

1 water with a residual pressure of 98 kPa under vacuum saturation for 20 min. After that, the samples
2 were conditioned in a temperature environmental chamber at -18 °C for 16 hours. At last, the
3 samples were placed in distilled water at 25 °C and thawed for 12 hours.

4 A micro medical syringe pump was utilized to drop the moisture into asphalt mixture samples.
5 The flow rate was demarcated as 0.1 ml/min in this study. The details about this apparatus were
6 described in [31]. Penetration test were first conducted on the conditioned samples to analyze the
7 initial seepage characteristic. Then these samples were treated by 10 successive freeze-thaw cycles.
8 After 3, 6, and 9 freeze-thaw cycles, the penetration experiment performed on the damaged asphalt
9 mixtures to identify the evolution of seepage characteristic with exposure to freeze-thaw cycles.

10 *X-ray scanning and seepage characteristic determination*

11 Testing method is the key to describe the seepage characteristic. However, in previous analysis,
12 the quantitative measurements in microscale moisture distribution within samples were difficult to
13 perform. That hindered the discussions on the macroscale permeability [2, 32-35]. The micro-scale
14 seepage characteristics, mainly include local seepage velocity and wetting front position. But the
15 latter cannot be captured by traditional testing techniques. Recently, the X-ray nondestructive
16 determination technique has been widely utilized to capture inside moisture flow on mesoscopic
17 scale [20, 30]. Thus, X-ray CT system was used to image the dynamic flow in samples with exposure
18 to freeze-thaw cycles.

19 The development of an X-ray CT device makes it possible to picture the mesoscopic structure
20 inner asphalt mixture. However, due to the almost same density of moisture (0.95-1.04 g/cm³) and
21 asphalt binder (0.95-1.10 g/cm³), X-ray CT image exhibits the similar greyscale in these two
22 materials, and therefore it cannot extract directly the moisture from asphalt mixtures. In 2016, Xu

1 et al. [20] developed a non-void object increment method identify the moisture from asphalt
2 mixtures. The measurement error of this approach is within $\pm 6\%$, and therefore was selected and
3 applied in this study. In test, firstly, X-ray CT scanning was conducted to image the pore structure
4 of mixture in dry as the base of the non-void object increment method. An in-situ seepage test under
5 X-ray CT scanning was performed to capture the dynamic flow behavior inside the samples. The
6 images obtained during the seepage process were compared with the images in dry and the
7 difference of non-void part (aggregate and asphalt mortar) of initial images was determined as
8 moisture. The scanning time was 18 min, scanning current was 300 μA , and scanning voltage was
9 190 kV. The detailed procedural of non-void object increment method has been described according
10 to Xu et al. [31].

11 Parameters such as local directional seepage velocity, penetration depth, and wetting front,
12 have been successfully applied to describe the seepage characteristics in porous media. In the
13 analysis of seepage evolution under various pore structure and experimental temperature conditions,
14 the studies on the moisture propagation with soil samples have been widely conducted with
15 utilization of these parameters. That was successful to represent the seepage characteristics in
16 dynamic conditions.

17 In addition, the IIR depth is also a crucial property that helps understand the transfer of initial
18 inertia caused by moisture dropped from a needle in the asphalt mixtures. The IIR can be determined
19 by the variation rate of seepage velocity. In the IIR, inertia force is the dominant factor in infiltration,
20 and decreases with depth. In this region, the seepage velocity slows with inertia. In the INR, gravity
21 and capillary turn into the dominant factors instead of inertia. In this region, Darcy' law is applicable.
22 However, in INR, the seepage velocity of wetting front is almost constant because of the limited

length of the specimen. The depth of IIR is a means to divide the driving force for moisture movement in porous medium. A large IIR depth value indicates a small flow resistance, and a small IIR value indicates an increasing flow resistance.

In this study, the variations in the directional seepage characteristics of the asphalt mixtures were quantified by measuring the seepage velocity, penetration depth, and IIR depth. Penetration depth was measured based on the 2D scanning images using non-void object increment method, whereas the local directional seepage velocity was calculated from the penetration depth of adjacent time by using Eqs. (1) to (2). The IIR can be captured by the directional seepage velocity curves, and consequently, the IIR depth can be determined.

$$V_{\text{wetting front-Z direction}} = \frac{Z(t_i) - Z(t_{i-1})}{t_i - t_{i-1}} \quad (1)$$

$$V_{\text{wetting front-X direction}} = \frac{X(t_i) - X(t_{i-1})}{t_i - t_{i-1}} \quad (2)$$

Where $V_{\text{wetting front-Z direction}}$ and $V_{\text{wetting front-X direction}}$ are the vertical and horizontal seepage velocity, respectively. $Z(t_i)$ and $X(t_i)$ are the vertical depth and horizontal location of moisture penetration at (t_i) , respectively.

Results and discussion

Evolution of moisture wetting front in asphalt mixtures during freeze-thaw cycles

Wetting front

Wetting front is defined by Xu et al. [31] and Gong et al. [36] as the moisture leading edge of a porous material under saturated and unsaturated. It usually relies on the internal structure of the porous medium. Using the aforementioned analysis method, the wetting front in asphalt mixture samples can be captured quantitatively. This section qualitatively examines the moisture penetration in asphalt mixtures during freeze-thaw cycles. —The results from the various freeze-thaw

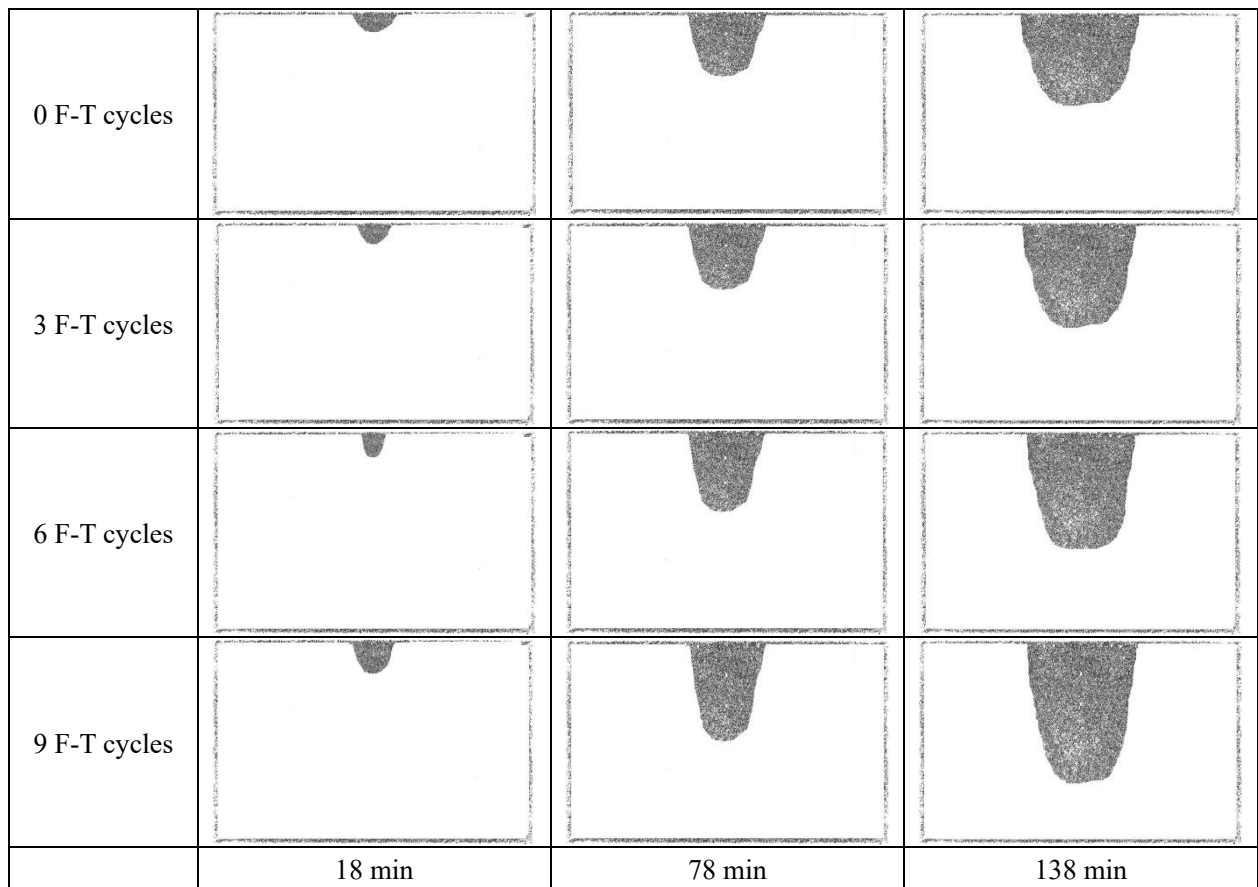
1 experiments exhibited the temporal evolution of moisture distribution, which shows in Fig. 1-3. The
2 section shown in figures were the vertical section cross the center of samples. The shadow in the
3 sections was the wetting area and the edge was defined as the wetting front.

4 The moisture infiltration process after 0, 3, 6, 9 freeze-thaw cycles was scanned with different
5 penetration time, namely, 18, 78, and 138 min. The initial moisture content was 0%. Generally, the
6 infiltration of moisture into asphalt was affected by inertia, capillary and gravity forces based on
7 three essential factors. The moisture movement in all directions is affected by capillary forces but
8 the vertical moisture is specially affected by gravity forces. For the AC mixture shown in Fig.1, for
9 instance, it can be clearly observed that for the asphalt mixtures without freeze-thaw cycles, the
10 infiltration pattern is hemispherical shape at the initial penetration process, and gradually transfers
11 into a rectangular shape with the increase of penetration duration. This phenomenon indicates the
12 existence of a driving force transformation during the infiltration process.

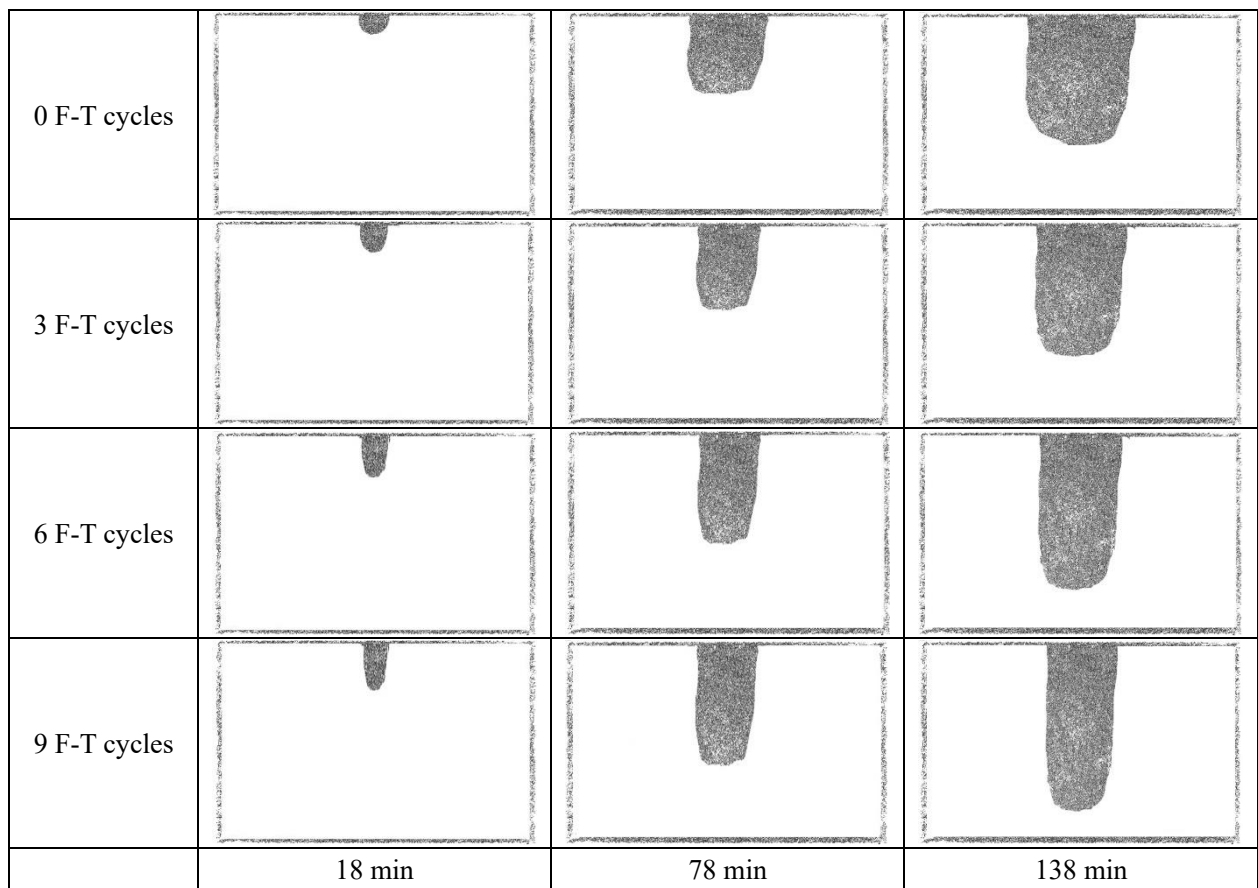
13 Particularly, based on the limited number of X-ray CT images, a general observation is difficult
14 to make, but the freeze-thaw cycle would be an acceleration to the transformation of infiltration
15 pattern. Regardless of the gradation of asphalt mixtures, it is interesting to observe that the wetting
16 front is shrinked in the horizontal direction and expanded in the vertical direction under the freeze-
17 thaw treatment. Under the effect of freeze-thaw action, this change is more obvious. This result
18 indicates the important function of freeze-thaw cycles on the wetting front in samples. To be more
19 specific, capillary and inertia force decreases in the horizontal direction and increases in the vertical
20 direction with increasing freeze-thaw cycles, and results in the infiltration pattern transformation.

21 The similar phenomenon happens in SMA and OGFC mixtures which shown in Figs.2-3. The
22 infiltration pattern evolved from a hemispherical shape to a rectangular shape with the conduction

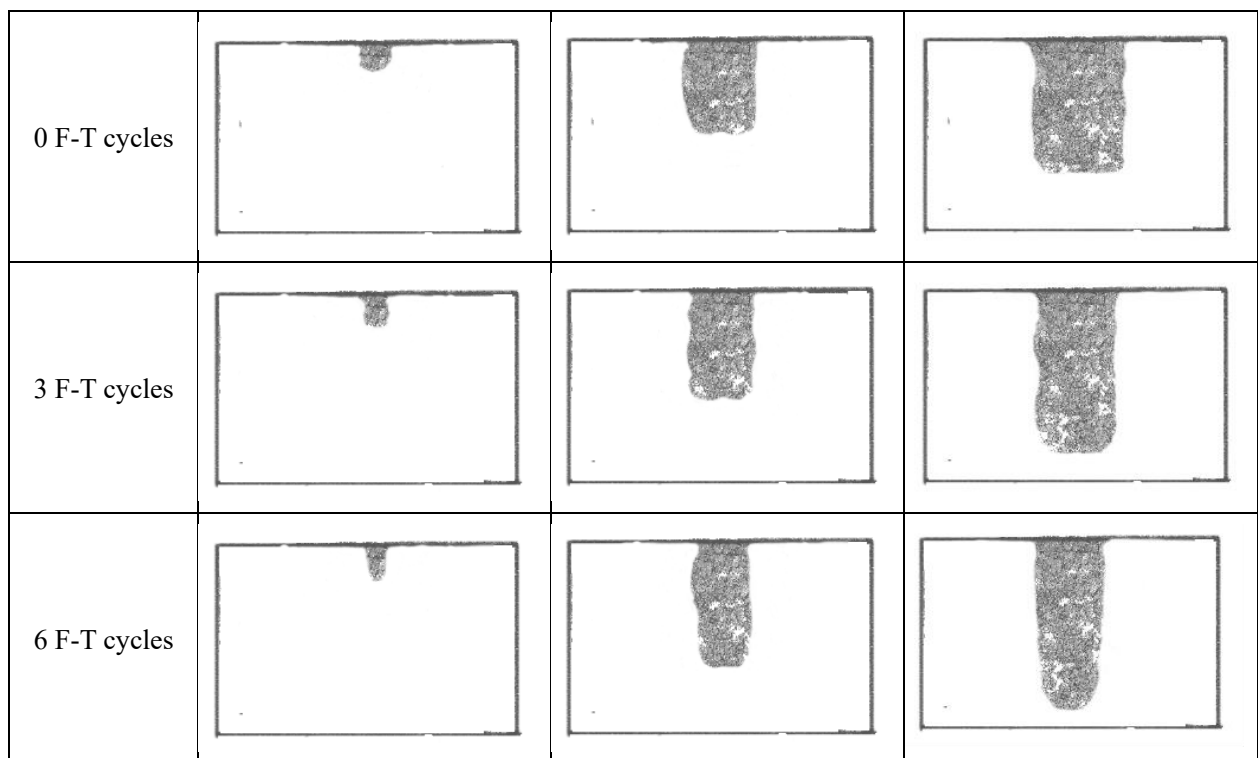
1 of penetration process. Also the wetting front shrank in the horizontal direction and expended in the
 2 vertical direction under the freeze-thaw treatment. However, regardless of the similar trend of
 3 moisture migration, the local velocity of wetting front was obviously different according to the
 4 varied mixture gradation. As can be seen in Fig.1-3, the wetting front in OGFC sample transferred
 5 faster in vertical direction compared to other two samples during the penetration process. And the
 6 expending of wetting front in vertical direction and shrinking of wetting front in horizontal direction
 7 were more obviously in OGFC. This phenomenon illustrates the significant impact of microstructure
 8 of asphalt mixture on moisture infiltration behavior under freeze-thaw cycles and would be
 9 discussed in later section of *The role of pore structure on seepage characteristic evolution with*
 10 *freeze-thaw cycles* in detailed.



11 Fig.1 Temporal evolution of moisture distribution under various freeze-thaw cycles (AC mixture)



1 Fig.2 Temporal evolution of moisture distribution under various freeze-thaw cycles (SMA mixture)



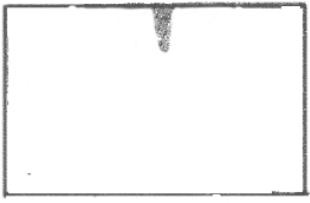
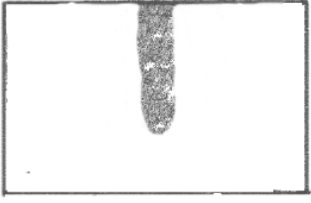
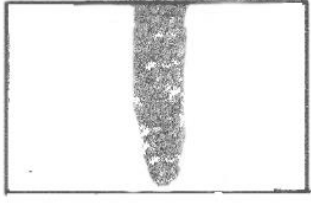
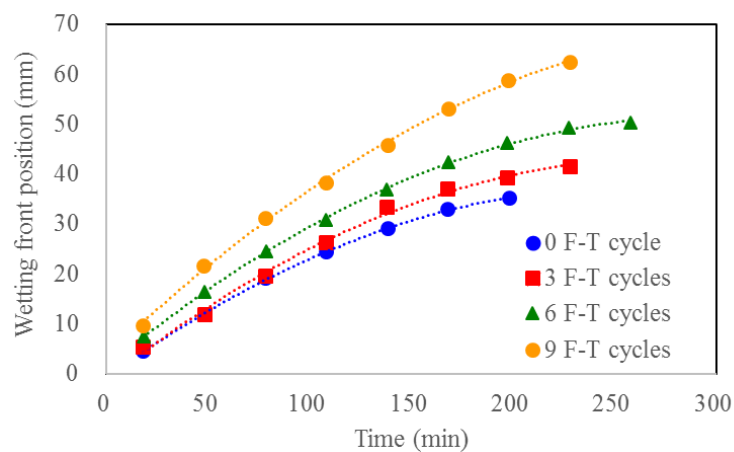
9 F-T cycles			
	18 min	78 min	138 min

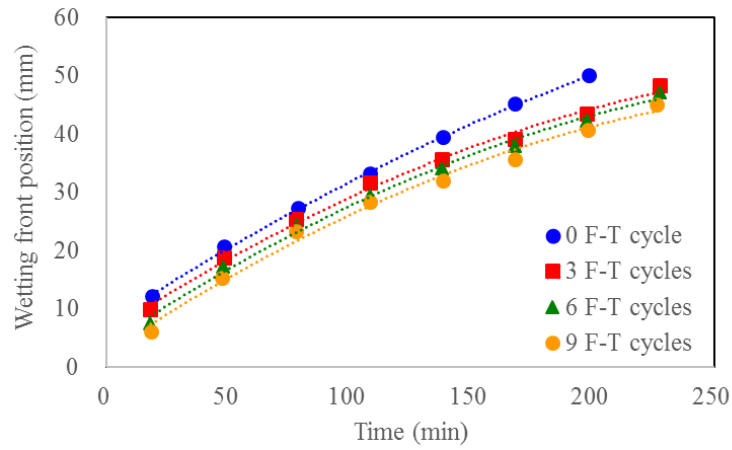
Fig.3 Temporal evolution of moisture distribution under various freeze-thaw cycles (OGFC mixture)

Local velocity of wetting front

We notify the results of analysis of directional wetting front under various freeze-thaw cycles and internal structure according to the previously described analysis procedures. One specimen from each type of asphalt mixture was chosen to demonstrate the effect of freeze-thaw cycles on the wetting front evolution. The vertical wetting front distance was measured based on the transmission of moisture from the horizontal surface plane of specimen, and the horizontal wetting front analysis was carried on based on the vertical plane that was perpendicular to the incidence direction of X-ray and passed through the incident point (center of the circle). The measured temporal wetting fronts in different asphalt mixtures with and without freeze-thaw actions are shown in Figs. 4-6.

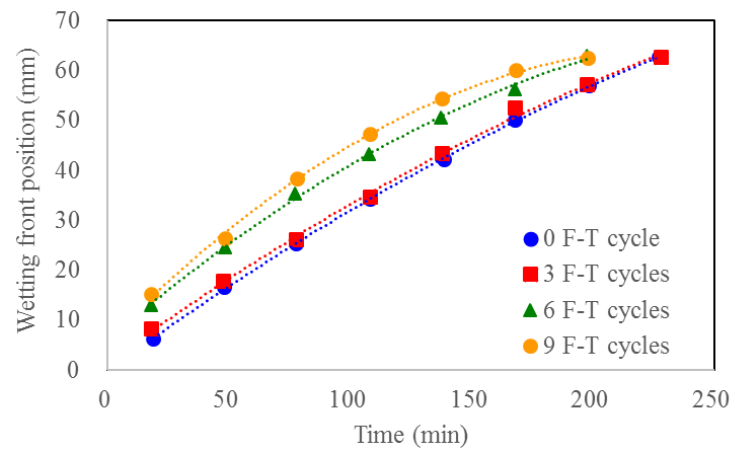


(a) Vertical direction

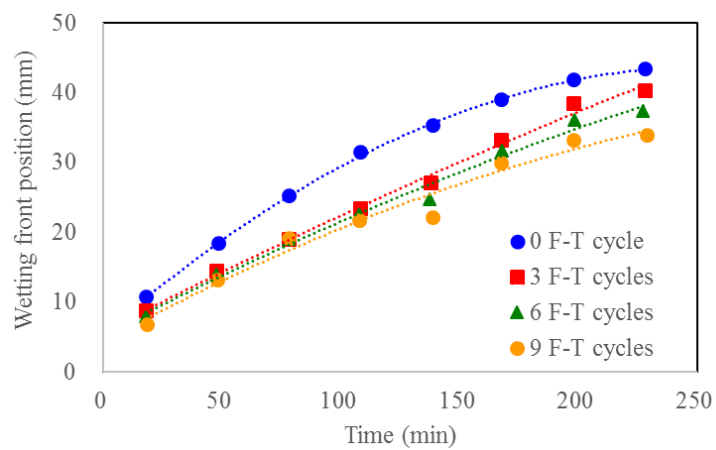


(b) Horizontal direction

Fig. 4 Temporal variation of wetting front position under various freeze-thaw cycles (AC mixture)

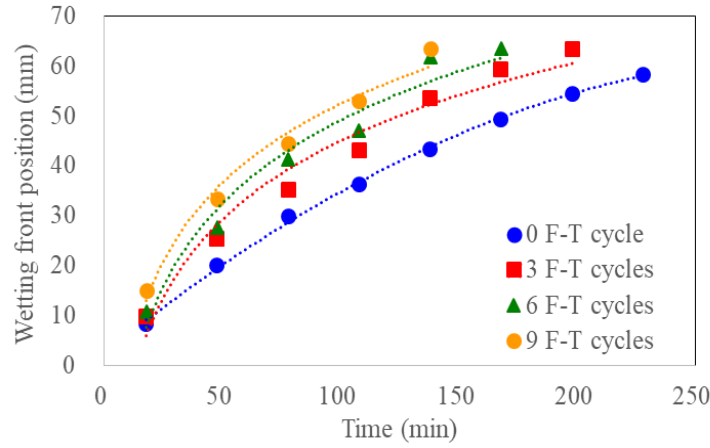


(a) Vertical direction

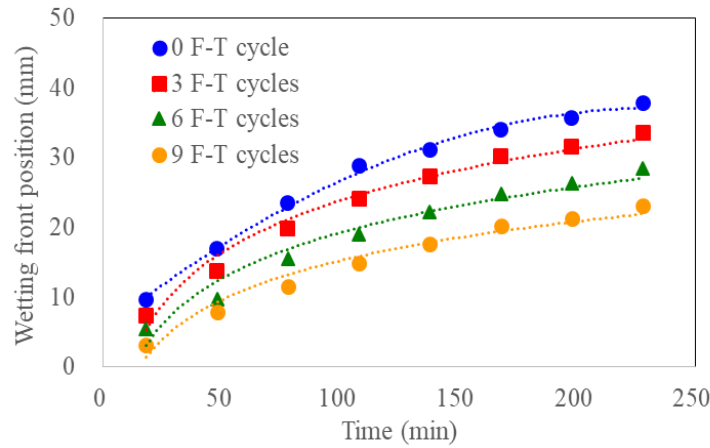


(b) Horizontal direction

Fig. 5 Temporal variation of wetting front position under various freeze-thaw cycles (SMA mixture)



(a) Vertical direction



(b) Horizontal direction

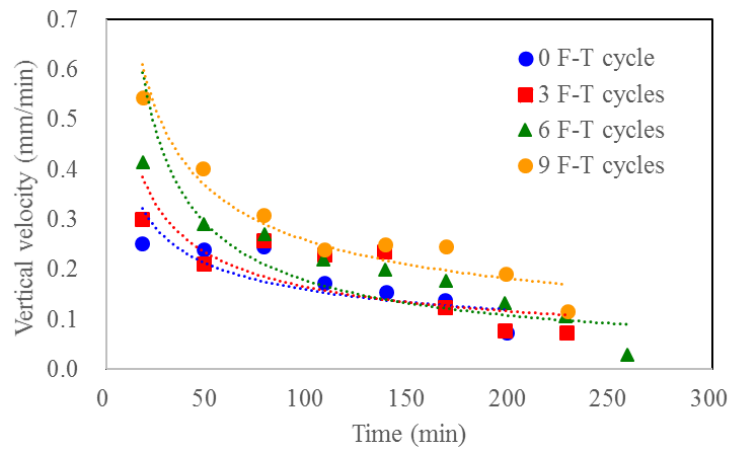
Fig. 6 Temporal variation of wetting front position under various freeze-thaw cycles (OGFC mixture)

The blue, red, green, and orange curves describe the wetting front positions in asphalt mixtures after 0, 3, 6, and 9 freeze-thaw cycles, respectively. A larger wetting front position denotes more involved pores that lead to moisture penetration into the samples. In Figs. 4-6, regardless of asphalt mixture type, although all the penetration times in the test are at the same level, the vertical wetting front position in the sample moved up with the intensifying of freeze-thaw action. For instance, with the penetration time of 138 min, the wetting front in the original AC mixture locates at 29 mm below the top surface, while the samples with 9 freeze-thaw cycles is 46 mm. The latter exhibits an extra penetration depth of 17 mm due to the damage of freeze-thaw action. Contrary to the vertical wetting

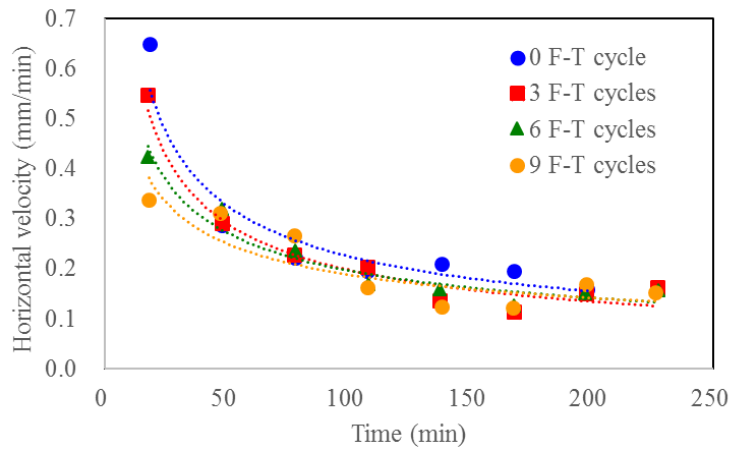
1 front, the horizontal wetting front position decreases with intensifying of freeze-thaw action. Fig.
2 4(b), 5(b) and 6(b) show that with the freeze-thaw cycles circulating from 0 to 9, the penetration
3 depth at 138 min is decreased by 18% for AC mixture, 37% for SMA mixture, and 44% for OGFC
4 mixture. This phenomenon illustrates an increase in vertical flow penetration and a decrease in
5 horizontal flow penetration under freeze-thaw cycles. In other words, freeze-thaw cycle aggravates
6 the anisotropy of seepage in samples.

7 The directional velocity variations, as shown in Fig 7-9, were obtained from the data pair of
8 penetration time versus wetting front position that is shown in Figs. 4-6. It is obvious that freeze-
9 thaw cycles make a significant difference in directional velocity at the early stage of infiltration,
10 while the difference caused by freeze-thaw cycles is very weak in the later infiltration. This
11 phenomenon illustrates that the influence on the directional velocity resulted from freeze-thaw cycle
12 is mainly in the early stage of infiltration, and has a very slight impact on the later stage of infiltration.
13 In particular, the evolution of velocity with freeze-thaw cycles, which shown in Fig.7-9, indicates
14 the of anisotropy changes in the directional velocity. Although the penetration time and penetration
15 rate for the experiment were applied at the same level, the variation of vertical velocity with the
16 freeze-thaw action was opposite to that of the horizontal velocity. Specifically, the penetration
17 vertical velocity increases with freeze-thaw cycles circulating. For instance, when the penetration
18 time is 18 min, compared with the cases free from freeze-thaw action, the vertical velocity under 9
19 freeze-thaw cycles is increased to 216% for AC mixtures, 253% for SMA mixtures, and 181% for
20 OGFC mixtures. However, the horizontal velocity always decreases with intensifying of freeze-
21 thaw cycles. When the penetration time is 18 min, the horizontal velocities without freeze-thaw
22 cycles are 0.65 mm/min for AC mixture, 0.59 mm/min for SMA mixture, and 0.54 mm/min for

1 OGFC mixture, while given 9 freeze-thaw cycles, the horizontal velocities is 0.34 mm/min, 0.38
2 mm/min, and 0.17 mm/min, respectively. The latter shows a horizontal velocity that is 36%~48%
3 slower than that in the former. This phenomenon indicates the anisotropic distribution feature of
4 directional velocity under freeze-thaw cycles and verifies the conversion of transport pattern
5 exhibited in Figs. 1-3.

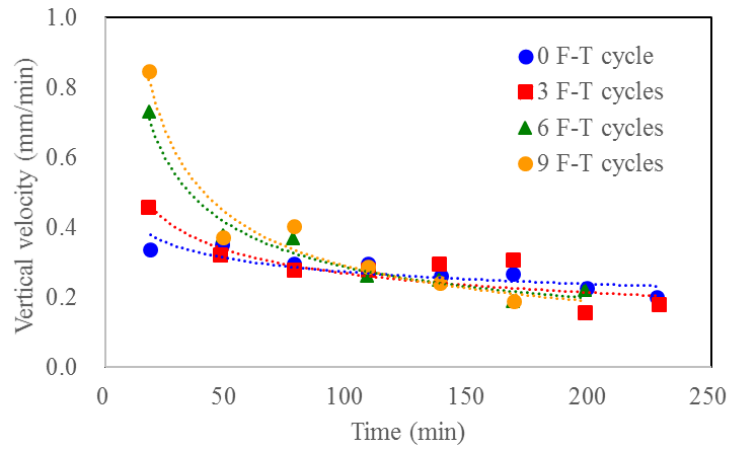


(a) Vertical direction

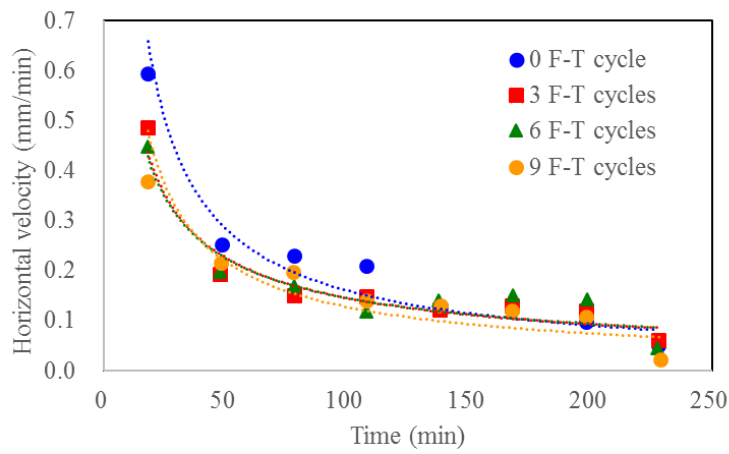


(b) Horizontal direction

Fig. 7 Temporal variation of seepage velocity under various freeze-thaw cycles (AC mixture)

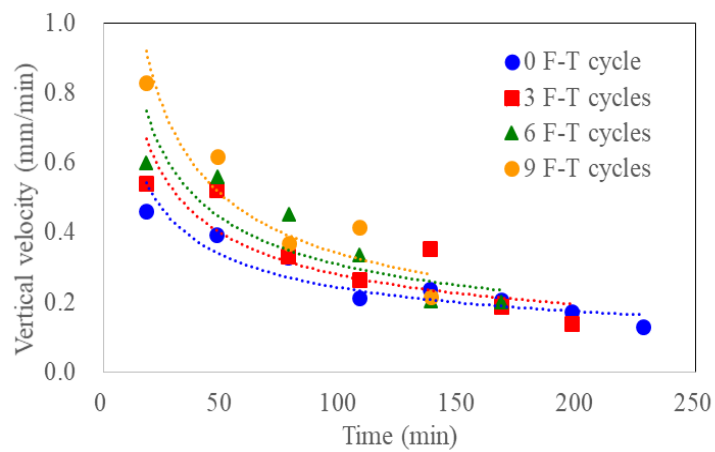


(a) Vertical direction

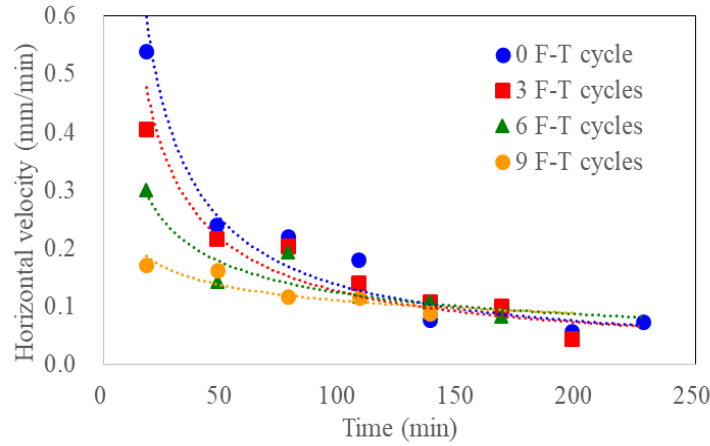


(b) Horizontal direction

Fig. 8 Temporal variation of seepage velocity under various freeze-thaw cycles (SMA mixture)



(a) Vertical direction



(b) Horizontal direction

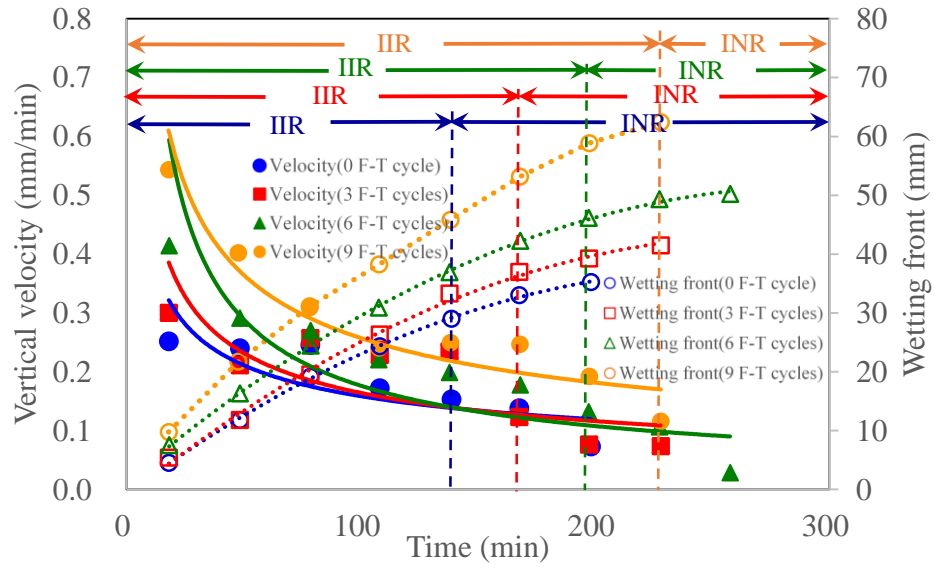
Fig. 9 Temporal variation of seepage velocity under various freeze-thaw cycles (OGFC mixture)

Inertia influence region

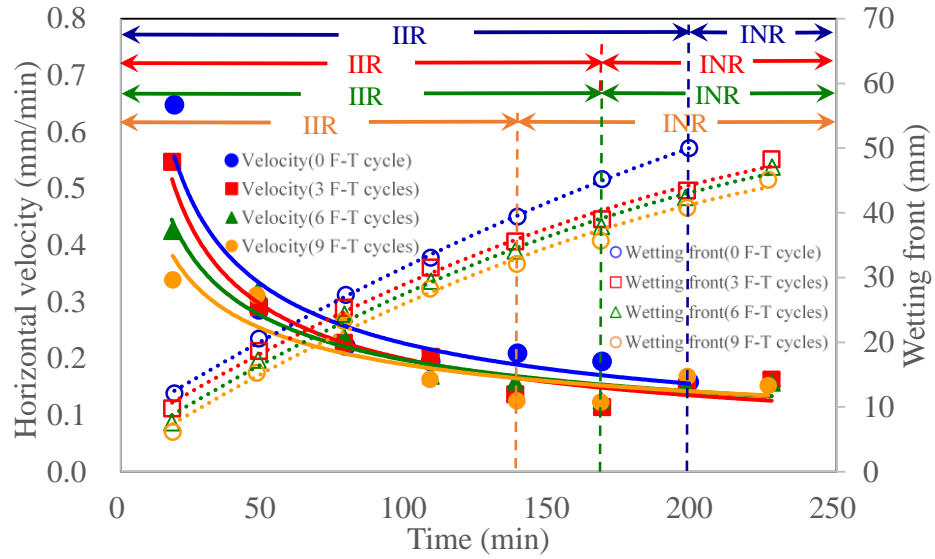
The water dropped from a needle has an initial inertia, in addition to gravity and capillary in the region of the point of impingement. According to the dominant force, the region through which water flows are distinguished to the IIR and the INR. In the IIR, by definition, inertia force is dominant to drive the moisture movement and the seepage velocity decreases with penetration monotonously. In the INR, instead of inertia force, gravity and capillary play crucial roles, and Darcy's law is applicable. In this zone, the seepage velocity remained almost constant and the wetting front migrated as a linear trend. As suggested by Jung et al. [37], the IIR and INR in porous medium can be determined from the data pair of penetration versus directional seepage velocity by considering the seepage velocity change. The critical boundary of this two zones in this paper was defined as the penetration time of decrease velocity of seepage velocity below 0.001 mm/min^2 . The evolutions of IIR for different samples under freeze-thaw cycles are shown in Figs. 10-12.

Figs. 10-12 illustrate the importance of freeze-thaw cycles on the dominant driving force in samples. Regardless of asphalt mixture type, the IIR along samples vertical direction increases with the cyclic freeze-thaw actions, whereas IIR along horizontal direction decreases gradually.

1 Specifically, according to the wetting front at the boundary between IIR and INR, it can be observed
2 that the vertical IIRs of these three types of asphalt mixtures increase 28.1 mm to 38.5 mm after 9
3 freeze-thaw cycles, compared with cases without freeze-thaw cycles. And the lasting time prolongs
4 120 min for AC mixture, 90 min for SMA mixture, and 60 min for OGFC mixture in the vertical
5 direction. On the other hand, in the horizontal direction, at the infiltration rate of 0.1 mm/min, the
6 IIR for AC mixture is 50.0 mm without freeze-thaw cycles, whereas that of 9 freeze-thaw cycles is
7 32.1 mm. The former exhibits an IIR in AC mixture that is 1.56 times more than that in later. The
8 similar change happened in other two types asphalt mixture and that is 1.74 times for SMA mixture
9 and 2.33 times for OGFC mixture. Meanwhile, the lasting time decreases from 198 min to 138 min
10 in AC mixture and from 168 min to 108 min in SMA and OGFC mixture due to the damage caused
11 by the freeze-thaw action. These phenomenon all illustrated a transformation for the IIR expanding
12 in vertical direction but shrinking in horizontal direction with freeze-thaw cycles. As suggested by
13 Xu et al. [2], the aggregation of existing voids to form micro-cracks is the dominant degradation
14 pattern during the initial freeze-thaw cycles. This process provides more channels in the vertical
15 direction for the flow to pass. Thus, due to the extension of flow path under freeze-thaw cycles, the
16 initial inertia is migrated to vertical direction under the intensifying of freeze-thaw action.

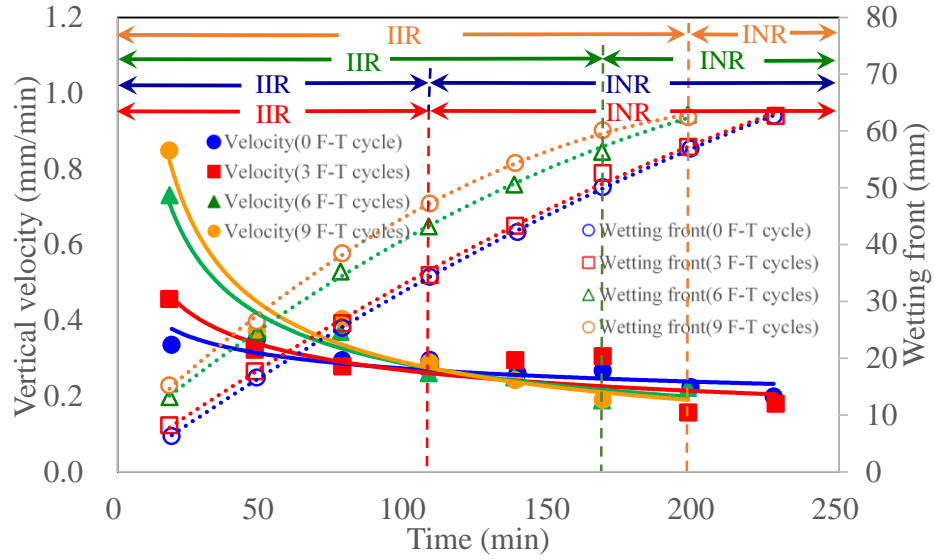


(a) Vertical direction

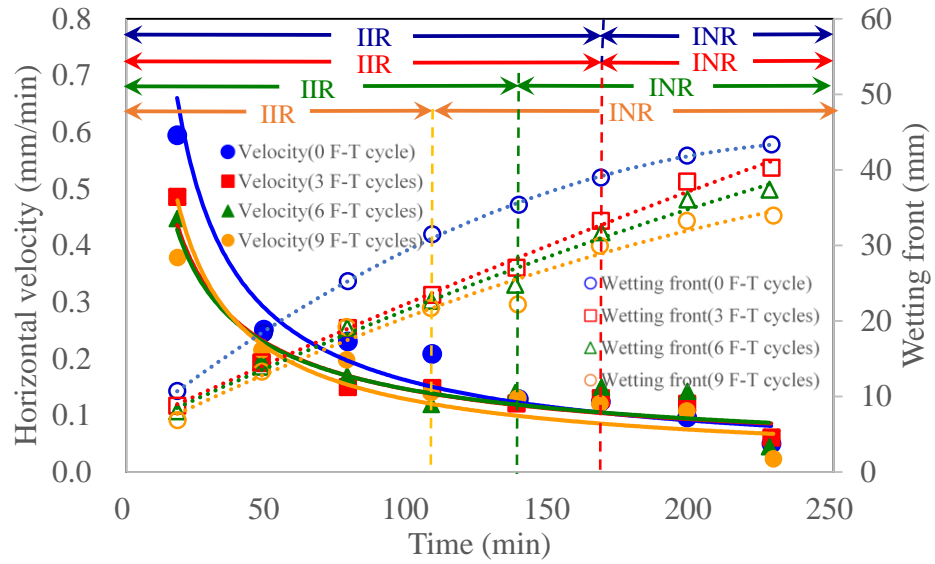


(b) Horizontal direction

Fig.10 Inertia influence region under various freeze-thaw cycles in AC mixture

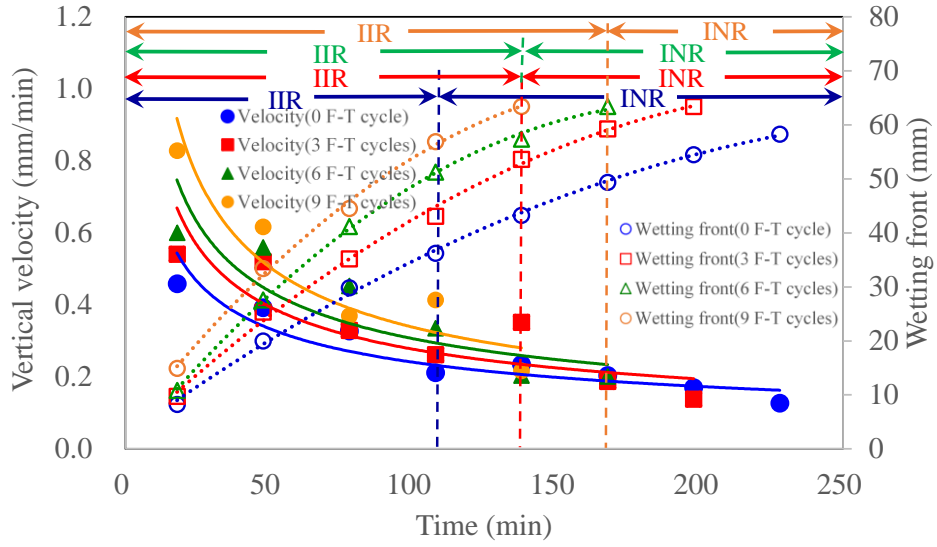


(a) Vertical direction

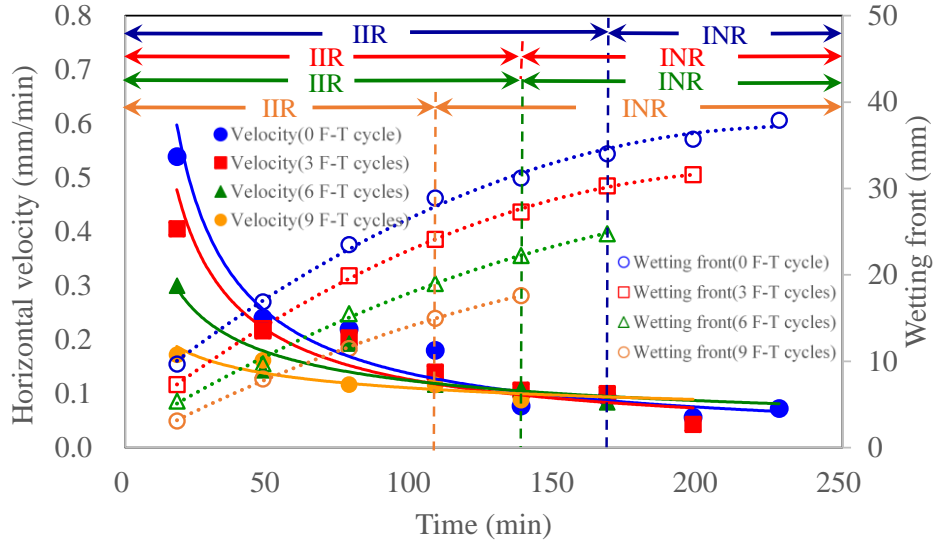


(b) Horizontal direction

Fig.11 Inertia influence region under various freeze-thaw cycles in SMA mixture



(a) Vertical direction



(b) Horizontal direction

Fig.12 Inertia influence region under various freeze-thaw cycles in OGFC mixture

The role of pore structure on seepage characteristic evolution with freeze-thaw cycles

Fig.13 shows directional velocity growth rates, in both vertical and horizontal direction, at various freeze-thaw cycles for different asphalt mixtures. For the two data pairs shown in Fig.13, the change of directional velocity growth rate under freeze-thaw action can be approximately described as a linear relationship. Specifically, the number of freeze-thaw cycle has a positive effect

1 on the vertical seepage velocity growth rate, but a negative effect on horizontal seepage velocity

2 growth rate. Furthermore, the sensitivity of seepage velocity change to the freeze-thaw cycles to the

3 pore structure could be reflected by the slopes of the regression lines. A big slope represents a large

4 variation of seepage velocity growth rate, suggesting a high sensitivity to the freeze-thaw action.

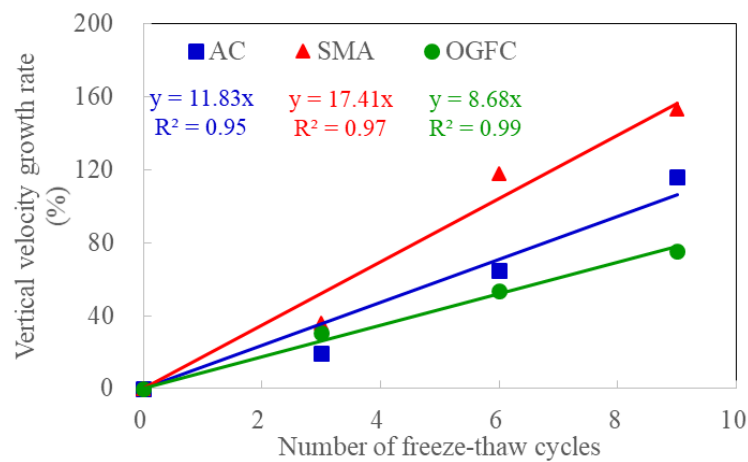
5 Clearly, dense-graded asphalt mixtures, such as AC and SMA mixtures, exhibit bigger slope for

6 vertical velocity, which is approximately 0.5 to 1 times more susceptible than OGFC mixtures. On

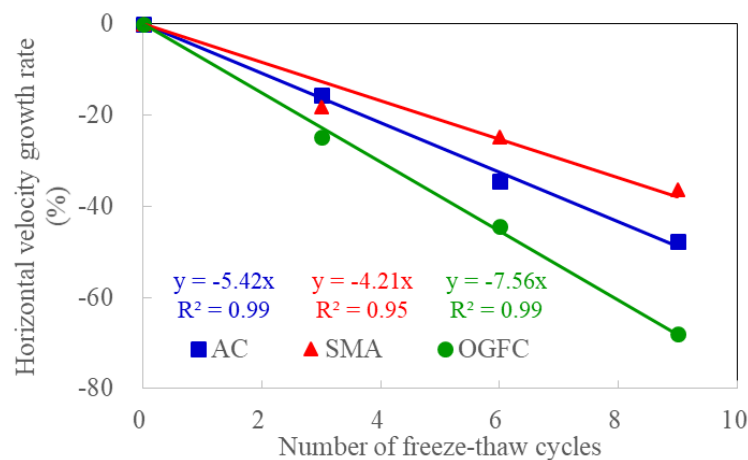
7 the contrary, for the horizontal velocity, the open-graded asphalt mixture OGFC, illustrates the

8 highest slope. This phenomenon indicates the significant role of pore structure in seepage velocity

9 evolution under freeze-thaw action.



(a) Vertical direction



(b) Horizontal direction

Fig.13 Directional seepage velocity growth rate versus number of freeze-thaw cycles

Conclusions

This study investigated the dynamic flow behavior in asphalt mixtures with freeze-thaw cycles. Two dense-graded asphalt mixtures and one open-graded asphalt mixture were evaluated through laboratory testing. A micro medical syringe pump was used to drop water and penetrate into asphalt mixture, and X-ray CT tests were conducted to capture the moisture migration through asphalt mixtures. The dynamic flow behavior in asphalt mixture were determined after 0, 3, 6, and 9 freeze-thaw cycles. The mainly conclusions of this study are summarized as follows.

Seepage characteristics in asphalt mixtures, such as wetting front position, directional velocity, and IIR, were adopted to quantify the evolution of dynamic behaviors under freeze-thaw cycles. It was found that the wetting front penetration depth and local velocity for vertical flow are increased, while those for horizontal flow are decreased under the intensifying of freeze-thaw action. This phenomenon indicated the exacerbation of seepage anisotropy in studied samples. Meanwhile, freeze-thaw cycles prompted more initial inertia of water droplet to transfer toward the vertical direction, and leading to the transformation of the infiltration pattern from hemispherical to slender at a specific infiltration time under freeze-thaw action.

An approximate linear regression equation was proposed to describe the sensitivity of directional velocity growth rate in asphalt mixture exposed to freeze-thaw cycles to pore structure. The number of freeze-thaw cycle has a positive effect on the vertical seepage velocity growth rate, but negative effect on horizontal seepage velocity growth rate. Large slope for vertical velocity and small slope for horizontal can be observed with the reduction of pore sizes. Thus, for the AC and SMA mixtures with small pore size, the velocity growth rate tends to rise rapidly in vertical direction and decrease slowly in horizontal direction under freeze-thaw cycles.

Acknowledgments

Funding from the Natural Science Foundation of China (Grant No. 51678207, 51608154) and the Fundamental Research Funds for the Central Universities (Grant No. HIT.BRETIII.201511) are gratefully acknowledged. The authors thank Yunliang Li for their assistances in the experiment process. Thanks to the anonymous reviewers for their comments that have notably helped us improve the manuscript.

References

- [1]T. You, R.K. Abu Al-Rub, E.A. Masad, D.N. Little, Three dimensional microstructural modelling of asphalt concrete by use of X-ray computed, Transportation Research Record. 2373 (2013) 63-70.
- [2]H.N. Xu, W. Guo, Y.Q. Tan, Permeability of asphalt mixtures exposed to freeze-thaw cycles, Cold Regions Science and Technology. 123 (2016) 99-106.
- [3]X.B Gong, P. Romero, Z.J. Dong, D.S. Sudbury, The effect of freeze-thaw cycle on the low-temperature properties of asphalt fine aggregate matrix utilizing bending beam rheometer, Cold Regions Science and Technology. 125 (2016) 101-107.
- [4]M.R. Hainin, N.I.M. Yusoff, M.K.I. Satar, E.R. Brown, The effect of lift thickness on permeability and the time available for compaction of hot mix asphalt pavement under tropical climate condition, Construction and Building Materials. 48 (2013) 315-324.
- [5]S. Caro, E. Masad, A. Bhasin, D.N. Little, Moisture susceptibility of asphalt mixtures, Part 1: mechanisms, International Journal of Pavement Engineering. 9(2) (2008) 81-98.
- [6]Y.P. Chen, M.S. Shi, X.C. Li, Experimental investigation on heat, moisture and salt transfer in soil, International Communications in Heat and Mass Transfer. 33 (2006) 1122-1129.

- 1 [7]Y.N. Zhang, L.B. Wang, B. Diefenderfer, W. Zhang, Determining volumetric properties and
2 permeability of asphalt-treated permeable base mixtures, *International Journal of Pavement*
3 *Engineering*. 17(4) (2016) 343-352.
- 4 [8]P.J. Vardanega, State of the Art: Permeability of asphalt concrete, *Journal of Materials in Civil*
5 *Engineering*. 26 (2014) 54-64.
- 6 [9]A. Benedetto, A. Umiliaco, Evaluation of hydraulic permeability of open-graded asphalt mixes
7 using a full numerical simulation, *Journal of Materials in Civil Engineering*. 26 (2014) 599-606.
- 8 [10]S. Saison, S. Wongwises, Two-phase air-water flow in micro-channels: An investigation of the
9 viscosity models for pressure drop prediction, *International Communications in Heat and Mass*
10 *Transfer*. 38 (2011) 212-217.
- 11 [11]J. Chen, T. Tang, Y.Q. Tang, Laboratory characterization of directional dependence of
12 permeability for porous asphalt mixtures, *Materials and Structures*. 50(5) (2017) 215.
- 13 [12]J.W. Meissner, N. Mendes, K.C. Mendonca, L.M. Moura, A full-scale experimental set-up for
14 evaluating the moisture buffer effects of porous material, *International Communications in Heat*
15 *and Mass Transfer*. 37 (2010) 1197-1202.
- 16 [13]M. Awadalla, A.O. Abd El Halim, Y. Hassan, I. Bashir, F. Pinder, Field and laboratory
17 permeability of asphalt concrete pavements, *Canadian Journal of Civil Engineering*. 44(4) (2017)
18 233-243.
- 19 [14]M. Ahmad, R.A. Tarefder, Critical permeability values of asphalt concrete for field cores and
20 laboratory-compacted samples, *Journal of Transportation Engineering Part B-Pavements*. 143
21 (2017) 04017013.
- 22 [15]H.N Xu, W. Guo, Y.Q. Tan, Internal structure evolution of asphalt mixtures during freeze-thaw

cycles, Materials and Design. 86 (2015) 436-446.

[16]H.N. Xu, H.Z. Li, Y.Q. Tan, L.B. Wang, Y. Hou, A micro-scale investigation on the behaviors of asphalt mixtures under freeze-thaw cycles using entropy theory and a computerized tomography scanning technique, Entropy. 20 (2018) 68.

[17]A.M. Kruse, M. Darrow, S. Akagawa, Improvements in measuring unfrozen water in frozen soils using the pulsed nuclear magnetic resonance method, Journal of Cold Region Engineering. 32 (2018) 04017016.

[18]P. Conte, V. Ferro, Measuring hydrological connectivity inside a soil by low field nuclear magnetic resonance relaxometry, Hydrological Processes 32 (2018) 93-101.

[19]E. Masad, B. Birgisson, A. Al-Omari, A. Cooley, Analytical derivation of permeability and numerical simulation of fluid flow in hot-mix asphalt, Journal of Materials in Civil Engineering. 16 (2004) 487-496.

[20]H.N. Xu, Y.Q. Tan, X.A. Yao, X-ray computed tomography in hydraulics of asphalt mixtures: Procedure, accuracy, and application, Construction and Building Materials. 108 (2016) 10-21.

[21]D. Castillo, S. Caro, M. Darabi, E. Masad, Modelling moisture-mechanical damage in asphalt mixtures using random microstructures and a continuum damage formulation, Road Materials and Pavement Design. 18 (2017) 1-21.

[22]J. Chen, T. Tang, Y.Q. Zhang, Laboratory characterization of directional dependence of permeability for porous asphalt mixtures, Materials and Structure. 50 (2017) 215.

[23]J.Q. Gao, C.C. Guo, Y.T. Liu, Measurement of pore water pressure in asphalt pavement and its effects on permeability, Measurement. 62 (2015) 81-87.

[24]P.J.Vardanega. State of the art: permeability of asphalt concrete, Journal of Materials in Civil

1 Engineering. 26 (2014) 54-64.

2 [25]X.D.Guo, M.Z. Sun, W.T. Dai, Analysis of effective pore pressure in asphalt pavement based

3 on computational fluid dynamics calculation, Advances in Mechanical Engineering. 9 (2017)

4 1687814016685224.

5 [26]S. Taniguchi, J. Otani, M. Kumagai, A study on characteristics evaluation to control quality of

6 asphalt mixture using X-ray CT, Road Materials and Pavement Design. 15 (2014) 892-910.

7 [27]A.A. Rose, E. Arambula, T. Howell, C.J. Glover, An X-ray CT validated laboratory

8 measurement method for air voids distribution over depth in asphalt pavement: A step toward

9 simplified oxidation modeling, Petroleum Science and Technology. 32 (2014) 3020-3028.

10 [28]R. Khan, A.C. Collop, G.D. Airey, A.N. Khan, Asphalt damage characterization from cyclic test

11 and X-ray computed tomograph, Proceedings of the Institution of Civil Engineers-Transport.

12 166 (2013) 203-2013.

13 [29]R. Khan, A.C. Collop, G.D. Airey, A.N. Khan, Asphalt damage characterization from cyclic test

14 and X-ray computed tomography, Transport. 166 (2013) 203-213.

15 [30]I. Jerjen, L.D. Poulikakos, M. Plamondon, P. Schuetz, T. Luethi, A. Flisch, Drying of porous

16 asphalt concrete investigated by X-ray computed tomography, Physics Procedia. 69 (2015) 451-

17 456.

18 [31]H.N. Xu, C. Xing, H.Y. Zhang, H.Z. Li, Y.Q. Tan, Moisture seepage in asphalt mixture using

19 X-ray imaging technology, International Journal of Heat and Mass Transfer. 131 (2019) 375-

20 384.

21 [32]T.F. Fwa, E. Lim, K.H. Tan, Comparison of permeability and clogging characteristics of porous

22 asphalt and pervious concrete pavement materials, Transportation Research Record. 2511 (2015)

1 72-80.

2 [33]A.G. Seferoglu, M.T. Seferoglu, M.V. Akpinar, Investigation of the effect of recycled asphalt
3 pavement material on permeability and bearing capacity in the base layer, *Advances in Civil*
4 *Engineering*. (2018) 2860213.

5 [34]M. Ahmad, R.A. Tarefder, Critical permeability values of asphalt concrete for field cores and
6 laboratory-compacted samples, *Journal of Transportation Engineering Part B-Pavement*. 143
7 (2017) 04017013.

8 [35]Y.N. Zhang, L.B. Wang, B. Diefenderfer, W. Zhang, Determining volumetric properties and
9 permeability of asphalt-treated permeable base mixtures, *International Journal of Pavement*
10 *Engineering*. 17 (2016) 343-352.

11 [36]J.Y. Gong, J.Q. Hou, G.J. Li, T.Y. Gao, J.J. Sun, A lattice Boltzmann study of frost growth on a
12 cold surface, *International Communications in Heat and Mass Transfer*. 98 (2018) 116-124.

13 [37]S.Y. Jung, S.M. Lim, S.J. Lee, Investigation of water seepage through porous media using X-
14 ray imaging technique, *Journal of Hydrology*. 452-453 (2012) 83-89.